nature nanotechnology

LETTERS

PUBLISHED ONLINE: 26 JANUARY 2014 | DOI: 10.1038/NNANO.2013.290

Bacillus spores as building blocks for stimuli-responsive materials and nanogenerators

Xi Chen[1], L. Mahadevan[2,3,4], Adam Driks[5] and Ozgur Sahin[1,4]*

Materials that respond mechanically to external chemical stimuli have applications in biomedical devices, adaptive architectural systems, robotics and energy harvesting[1–5]. Inspired by biological systems, stimuli-responsive materials have been created that can oscillate[2], transport fluid[3], provide homeostasis[4] and undergo complex changes in shape[5]. However, the effectiveness of synthetic stimuli-responsive materials in generating work is limited when compared with mechanical actuators[6]. Here, we show that the mechanical response of *Bacillus* spores to water gradients exhibits an energy density of more than 10 MJ m^{-3}, which is two orders of magnitude higher than synthetic water-responsive materials[7,8]. We also identified mutations that can approximately double the energy density of the spores and found that they can self-assemble into dense, submicrometre-thick monolayers on substrates such as silicon microcantilevers and elastomer sheets, creating bio-hybrid hygromorph actuators[9,10]. To illustrate the potential applications of the spores, we used them to build an energy-harvesting device that can remotely generate electrical power from an evaporating body of water.

In plants and many other biological organisms, water-responsive structures accomplish vital tasks such as the ascent of sap and the dispersal and self-burial of seeds[11–15]. Because of their critical functions, these water-responsive structures could possibly exhibit high energy densities and therefore potentially serve as the building blocks for stimuli-responsive materials that are efficient energy converters and actuators. In this work, we investigated the potential of *Bacillus* spores to convert energy from water gradients and to serve as the building blocks for high-energy-density stimuli-responsive materials.

Bacillus spores are dormant cells that can withstand harsh environmental conditions for long periods of time and still maintain biological functionality[16] (Fig. 1a,b). Despite their dormancy, spores are dynamic structures. For example, *Bacillus* spores respond to changes in relative humidity by expanding and shrinking, changing their diameter by as much as 12% (refs 17–20). We used an atomic force microscope (AFM)-based experiment (Fig. 1c) to determine the energy density of individual spores as they respond to changes in relative humidity. By adjusting the force and relative humidity, we created a thermodynamic cycle in which individual spores pass through four stages (Fig. 1d). In stage I, the spores rest at low relative humidity (~20%). In stage II, the cantilever exerts a predetermined force (loading). In stage III, the spores are subjected to high relative humidity (~90%). Finally, in stage IV, the force is reduced back to zero. The cycle is completed on lowering the relative humidity.

Figure 1e presents experimentally measured force versus height curves as spores of two species (*Bacillus subtilis* and *Bacillus thuringiensis*) and of a *B. subtilis* strain bearing mutations in *cotE* and *gerE* (*B. subtilis cotE gerE*)[21] proceed through the thermodynamic cycle. The areas enclosed by the force versus height curves in Fig. 1e correspond to the amount of work done by the spores (on the order of 1 pJ). To estimate the energy density of the spores, it is necessary to determine the volume of the material contributing to work. However, because stresses are localized near the apex of the AFM tip, it is difficult to define the interaction volume. To account for the non-uniformity in stress and strain distributions, we approximated the spore geometry as a cylindrical object (diameter × length of ~0.7 × ~1.5 μm) indented by a spherical tip (radius of ~0.85 μm). We estimated the spore energy density by comparing the energy of indentation calculated for this geometry with a case in which the spore is uniformly compressed by a planar indenter with the same depth of indentation (see Supplementary Section 1 for details of the calculations; note that the spore diameters used in these calculations are based on values determined experimentally with AFM height measurements). The resulting estimates of the energy densities and their standard deviations are plotted in Fig. 1f together with the maximum strains corresponding to the relative changes in spore diameter.

We note that the spores studied here showed differences in both energy densities and strain responses. In particular, the differences in energy densities between *B. subtilis* (10.6 MJ m^{-3}) and the other two spores (*B. subtilis cotE gerE*, 19.2 MJ m^{-3}; *B. thuringiensis*, 21.3 MJ m^{-3}) are statistically significant (mean values are separated by more than four standard deviations). These differences can be partially explained by the relative size and swelling ability of the cortex layers in each species. For example, the *B. subtilis cotE gerE* mutant spore lacks most of its coat layers[21], thereby reducing the volume of the spore contributed by the coat and increasing the relative cortex volume (Fig. 1b). These effects may explain the increase in strain response and energy density due to these mutations. We also note that the maximum forces we could reversibly apply to the spores were consistently higher for *cotE gerE* mutant spores than wild-type spores, which also contributed to the relative increase in energy density of these mutants. This favourable outcome suggests that an improved understanding of the hierarchical spore ultrastructure under extreme forces[22] can facilitate the use of genetic manipulation to allow further increases in energy density and strain responses. Note that improving the physical characteristics of materials through genetic manipulation has been successfully utilized in related areas like virus-based electromechanical conversion and material synthesis[23,24], highlighting the distinct advantage of using biologically based materials.

Because most of the water absorption and release in spores is due to the cortex, the energy density of the cortex alone is likely to be

[1]Department of Biological Sciences and Department of Physics, Columbia University, New York, New York 10027, USA, [2]School of Engineering and Applied Sciences, Department of Physics, Department of Organismic and Evolutionary Biology, Harvard University, Cambridge, Massachusetts 02138, USA, [3]Kavli Institute for Nanobio Science and Technology, Harvard University, Cambridge, Massachusetts 02138, USA, [4]Wyss Institute for Biologically Inspired Engineering at Harvard University, Boston, Massachusetts 02115, USA, [5]Department of Microbiology and Immunology, Loyola University Medical Center, 2160 S. First Avenue, Maywood, Illinois 60153, USA. *e-mail: sahin@columbia.edu

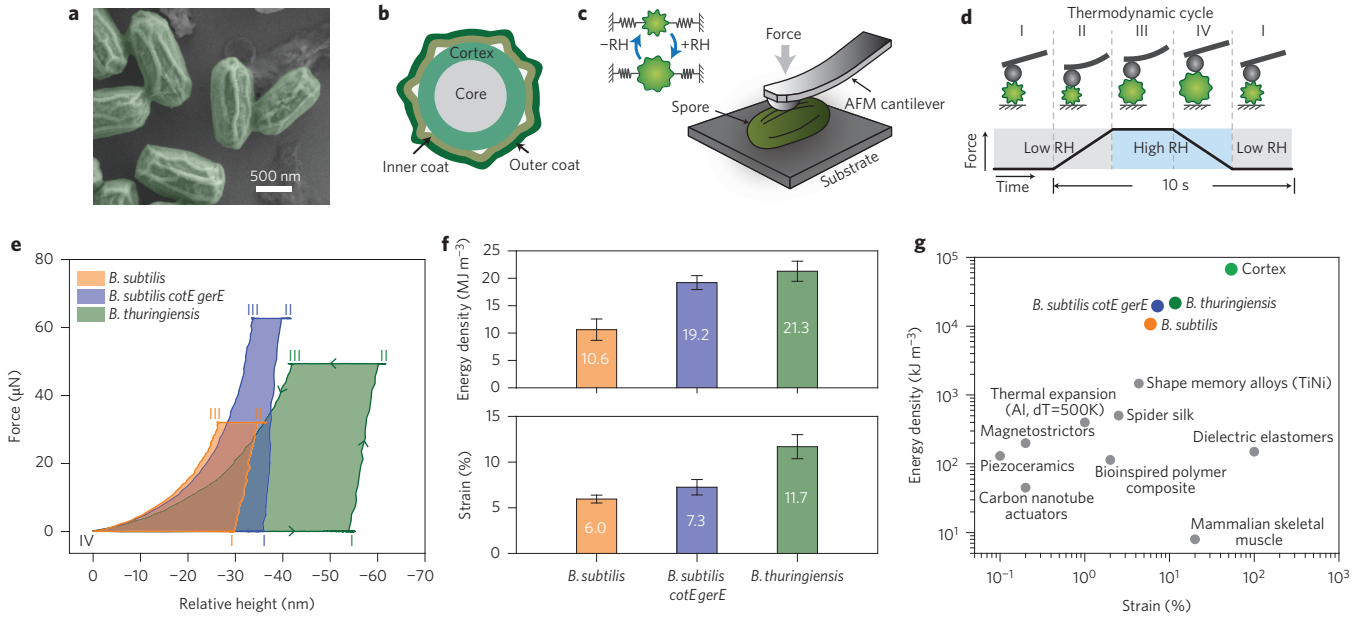

Figure 1 | High energy density of *Bacillus* spores. a, A false-coloured SEM image of *B. subtilis* spores. **b**, Spores are composed of multiple concentric shells encasing dehydrated genetic material at the centre (the core). One of these shells is a loosely crosslinked peptidoglycan layer, called the cortex, which can absorb water and swell, causing the coat to unfold[17–20]. **c**, Expansion and contraction of spores in response to changing relative humidity (RH) can potentially generate work that can be measured by AFM. **d**, Illustration of a thermodynamic cycle created by controlling the force and relative humidity. **e**, Force versus relative height curves during the thermodynamic cycle. **f**, Energy density and strain responses of different spore types. Standard deviations are calculated from measurements on five samples for each spore type. **g**, Comparison of the results in **f** with typical values reported for materials frequently used or studied in the context of actuators[6] and stimuli-responsive materials[7] (see Supplementary Table 1 for additional references and numerical values used to create **g**).

even higher than that for the entire spore. A simple estimate can be based on relative cortex volume, which could be obtained by approximating the coat and cortex layers as cylindrical shells encasing the core with respective thicknesses and radius of 60 nm, 60 nm and 200 nm (the numbers are estimated from cross-section transmission electron microscopy (TEM) images in ref. 20). These numbers result in a cortex energy density of 30–60 MJ m^{-3}. We also estimate the strain in the cortex to be ~50%, assuming that the majority of the diameter change is due to expansion of this layer. Figure 1g compares the estimated energy densities and strain responses of the spores and the cortex with typical values reported for materials frequently used or studied in the context of actuators and stimuli-responsive materials. As seen in this comparison, spores are remarkable actuators with extreme characteristics. We speculate that the origin of the high energy density lies in the nanoscale structure and material properties of the spores. Confinement of water in nanoscale pores of the spore cortex may be preventing water cavitation, which would create large negative pressures in water as a response to dehydration. At the same time, the high elastic modulus of the spores[20] may be preventing the collapse of the spore structure under large negative pressures, allowing them to change shape under high pressure.

The mechanical behaviour of individual spores suggests that they can serve as the building blocks for high-energy-density stimuli-responsive materials. The spores' small physical dimensions suggest that self-assembly may be sufficient to form approximate monolayers following the deposition and drying of a spore suspension on a substrate (Fig. 2a,b). With this approach, we assembled *B. subtilis* spores on silicon microcantilevers and latex rubber sheets, and observed their response to changes in water potential. We chose *B. subtilis* in part because of its lack of an additional outer layer, the exosporium, as is possessed by some species, and which might reduce the packing density[25]. The differential strain exerted by the spores caused a change in the curvatures of the microcantilevers and latex sheets, as shown in Fig. 2c,g. These deformations allowed us to characterize the response of the single-spore-thick layer to changes in water potential. We determined the curvature of the spore-coated latex sheet from images taken by a camera. However, because of the small sizes of the microcantilevers, we used an AFM to characterize the cantilever deformations by reflecting the laser from the uncoated surface (Fig. 2d,e).

Measurements with the spore-coated microcantilever demonstrated excellent reversibility and a relatively fast response to variations in water potential. Figure 2f shows the response of the microcantilever (width × length × thickness = 30 × 300 × 1.5 μm) to cyclical variations in relative humidity (15% versus 85%) before and after one million cycles. The data show that the spores initially moved the tip of the cantilever by 18 μm, which corresponds to a strain of ~0.04%. During this process, the spore layer generated a plane stress of 25.4 N m^{-1}. Following one million cycles of low and high relative humidity, the variations in tip deflection and in the corresponding surface stress reduced only slightly, demonstrating a high reversibility in the response of the spore monolayer. This reversibility is important for potential technological applications.

The data in Fig. 2f also show that the spores responded mechanically within ~0.4 s of exposure to humidity and within ~0.5 s of water release. This relatively fast response has important consequences for power output, and can be explained by the small thickness of the spore monolayer, where wetting and drying can occur very quickly. Quantitatively, both the classical Washburn law for wetting and diffusive evaporation for drying follow similar dynamical laws, with the time for both scaling as $\tau \approx h^2/D$, where h is the thickness of the sheet and D is the diffusivity[9,10]. Because power depends on these time constants, thinner films have a considerable advantage in terms of power.

The work done by spores to bend the underlying flexible substrate can be maximized by choosing optimal substrate materials

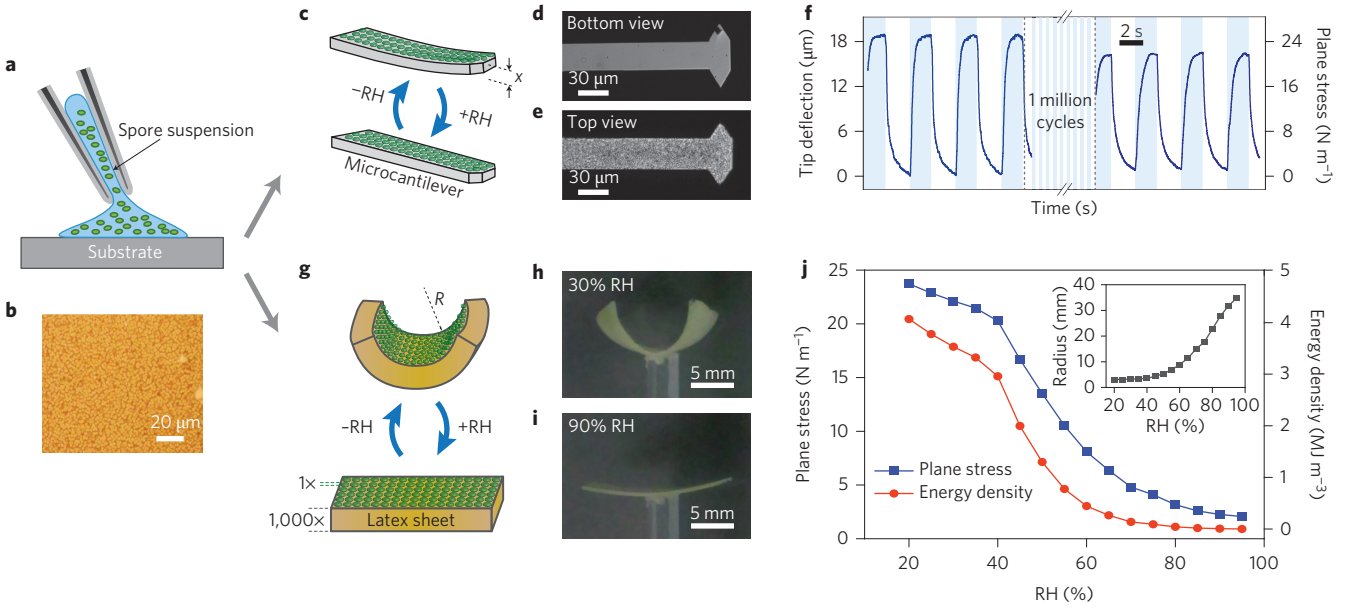

Figure 2 | Assembling spores into high-energy-density stimuli-responsive materials. a,**b**, Spores deposited onto a substrate (**a**) form a dense monolayer on drying, as seen using an optical microscope (**b**). **c**,**g**, Spores placed on silicon microcantilevers (**c**) and latex rubber sheets (**g**) induce differential strain to cause curvature. **d**,**e**, Optical micrographs of the bottom (**d**) and top (**e**) of a silicon AFM cantilever. **f**, Displacement of the cantilever tip and the corresponding surface stresses in response to changing relative humidity, recorded before and after 1 million cycles between 15 and 85% relative humidity. **h**,**i**, Photographs of the rubber sheet at 30% (**h**) and 90% (**i**) relative humidity. The sheet is viewed along its short dimension. **j**, Measured radius of curvature (inset), corresponding plane stresses at the spore/rubber interface and energy density of the spore layer plotted against relative humidity (RH).

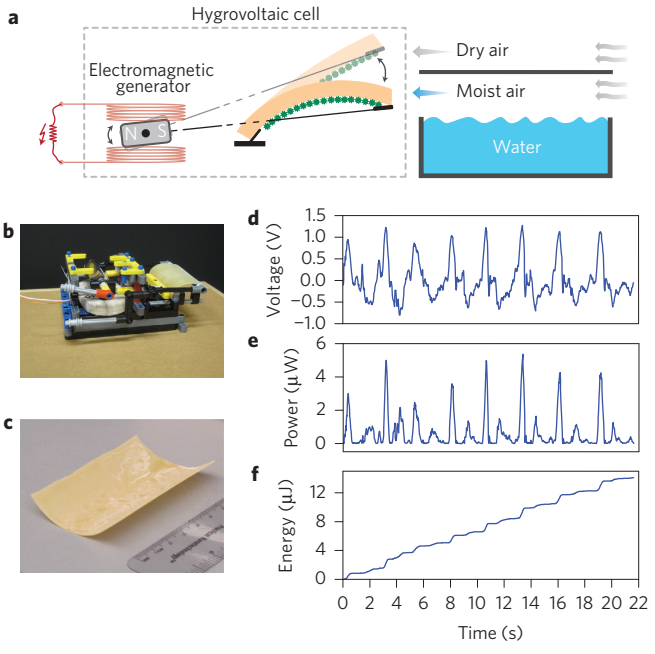

Figure 3 | Application of spore-based materials in energy harvesting. **a**, Schematic of the hygrovoltaic device. An electric fan was used to generate two streams of air (one flowing over the surface of the water and the other reaching the device directly) and a baffle was placed 1.5 cm above the water surface to direct the moistened air towards the generator. As the air reaching the device is switched between moist and dry, electrical energy is delivered to the load resistor. **b**, Photograph of the device used in the experiments. One of the two coils has been removed to expose the magnet. **c**, Photograph of the spore-coated latex sheet used in the experiment (width × length × height = 5 × 8 × 0.075 cm). **d**–**f**, Measurements of the voltage across the load (**d**), instantaneous power (**e**) and electrical energy delivered to the load (**f**).

and thicknesses. To identify the conditions that maximize energy output, we used a simple estimate for the maximum strain in a bilayer plate[9,10,26]. For a given ratio of the elastic moduli of the passive sheet and the spore layer, there is an optimum ratio of thicknesses that maximizes energy transfer (see Supplementary Section 2). Based on this analysis, we placed spores on 0.5-mm-thick latex rubber sheets and allowed the sheets to deform in a horizontal plane to minimize the effect of gravity in our analysis.

Varying the level of relative humidity produced dramatic changes in the shape of a 0.5-mm-thick rubber sheet coated with a single-spore-thick layer (Fig. 2h,i). From the observed radii of curvature we determined the surface stress and the energy density of the spore monolayer. At 20% relative humidity, the strain was 10.9% and the stress produced (23.7 N m^{-1}) corresponded to a free energy of ~2.6 J m^{-2} and a work density of ~3.94 MJ m^{-3} (assuming a thickness of 660 nm for the spore layer, which is the average diameter of *B. subtilis* measured by AFM). Additional preparations of samples showed that work densities more than 1.4 MJ m^{-3} can be obtained repeatedly. These values are fairly close to the estimates based on AFM measurements of individual *B. subtilis* spores (10.6 ± 1.92 MJ m^{-3}), suggesting that the assembly process largely preserved the actuation ability of spores. We have also observed that samples prepared with thicker latex sheets exhibit crack formation in the spore layer, suggesting that improvements in adhesion between neighbouring spores and between the spores and the substrate may allow the work density of the spore assembly to be increased.

To demonstrate a potential application of spore-based stimuli-responsive materials, we created an energy-harvesting device, the hygrovoltaic generator, which remotely generates electricity from evaporation from a standing body of water. For this, we coupled a spore-coated rubber sheet to an electromagnetic generator and placed the device next to an open container of water (Fig. 3a–c). When dry and moist streams of air were alternated, the spore-based hygromorph rotated the magnet back and forth, causing an alternating current to pass through the 300 kΩ load resistor

(Fig. 3d–f). During this process, the spores delivered an average power of ~0.7 μW, which is already comparable to vibrational energy harvesters[27]. Remarkably, however, only ~3 mg of bacterial spores were needed to generate this level of power. From this value, we estimate the corresponding specific electrical power of spores to ~233 mW kg^{-1}. We note that this value is device-dependent. For example, the efficiency of mechanical coupling between the active spore layer and the rotating magnet can affect the power output. Furthermore, any limitations on water vapour transport in and out of the spore layer can also affect power output. Accordingly, directly integrating spores with nanoscale piezoelectric materials like viruses[24] and piezoelectric nanogenerators[28] can potentially lead to substantial improvements in device performance.

Our estimates of energy densities suggest that spores are likely to be the highest-energy-density materials for generating mechanical work. Together with their ability to self-assemble into functional structures, the spores' uniquely effective capability for energy conversion may lead to novel stimuli-responsive materials for a wide range of applications including energy harvesting and storage and robotic actuation. Furthermore, the ease of cultivating morphologically diverse and environmentally benign spores of many *Bacillus* species[29] and the ability to adapt their material and mechanical properties through genetic manipulation may lead to stimuli-responsive materials with genetically defined, optimized characteristics.

Methods

Experimental set-up for rapid switching of relative humidity. A laboratory air source was used to supply two streams of air travelling through plastic tubing. One of the streams was saturated with water vapour by passing it through a bubbler. The other stream carried air at ~10–20% relative humidity at room temperature (~21 °C). A solenoid valve (SMC, NVFS) and a motorized arm were used to block the air from the tubes one at a time, switching at the frequency of a square wave supplied by a power MOSFET (NTD4960N). The drifts in height measurements due to a possible mismatch in the temperatures of the dry and humid air were minimized (~4 nm peak to peak) by focusing the air flow to a small region surrounding the cantilever. We also found that the relative humidity near the imaging area was affected by the temperature of the AFM head and the piezo-scanner, which were slightly above room temperature. We placed an electric fan behind the AFM head to reduce the temperature around the imaging area to ~23 °C.

AFM indentation of single spores. A commercial AFM (Multimode SPM, Nanoscope V controller and Signal access module, Veeco Instruments) was used for AFM experiments. The indentation depth was passively monitored with Labview (National Instruments) using a data acquisition card (NI-DAQ S-series 6115). Forces applied by the cantilever were controlled by offsetting the feedback set-point value of the AFM with an analogue-summing amplifier (SIM 980, Stanford Research Systems). We used cantilevers with large tip radii (~850 nm), measured by scanning electron microscopy (SEM), and large spring constants (~500 N m^{-1}; LTRH probes, Team Nanotec). Spring constants were calibrated against reference cantilevers (Applied Nanostructures, FCL probes) that were separately calibrated using the Sader method[30]. Spores were first inspected (by tapping-mode imaging using the same probes) for possible contaminants and the presence of exosporium (in the case of *B. thuringiensis*). Selected spores were indented in contact mode by controlling the feedback set-point value. We recorded cantilever deflection and vertical position signals with the data acquisition card. The work outputs of spores were maximized by adjusting the indentation speed and the duration of the humid state (stages II → III).

Coating the AFM cantilever with spores. An AFM cantilever chip (Veeco Instruments, HMX-S) was gently placed on a flat piece of silicon wafer while the cantilever stayed in contact with the surface of the wafer. A suspension of spores (~1 mm in diameter) in water was pipetted onto the cantilever under an optical microscope and allowed to dry. The cantilever surface was inspected by optical microscopy to ensure spore coverage of its surface.

Measurement of changes in plane stress and mass of the cantilever. The plane stress σ at the surface of an elastic substrate with thickness t, Young's modulus E and Poisson's coefficient ν is related to the radius of curvature r according to Stoney's formula[26]:

$$\sigma = \frac{E}{6(1-\nu)}\frac{t^2}{r} \quad (1)$$

This formula provides a good approximation if the film generating stress is significantly thinner than the substrate so that the bending stiffness of the film is negligible. Although the thickness of the spore layer is comparable to the cantilever, we assumed that it has a negligible bending stiffness because it is composed of objects with approximately circular cross-sections. A more general treatment of curvature can be found in ref. 9. The AFM allows measurement of the slope of the cantilever at the location of the laser spot, rather than measurement of the radius of curvature. However, r can be related to the slope θ if the position of the laser spot relative to the cantilever base x is known. Assuming a parabolic profile for the cantilever, the radius is given by $r = x/\theta$. The changes in the slope near the free end of the cantilever were measured to be well beyond the detector limits (saturation), so we placed the laser spot close to the cantilever base. The exact position of the laser spot was estimated by comparing the ratio of the thermal noise levels at this location and at a location near the free end of the cantilever, using the analytical expression for the mode shape of a rectangular cantilever beam. The thickness of the cantilever was determined to be 1.49 μm from the spring constant. We used $E \approx 130$ GPa and $\nu \approx 0.278$ for silicon (100). We neglected the effect of the reflective aluminium coating (40 nm) and assumed the entire cantilever was made of silicon.

Coating latex rubber sheets with spores. Natural latex rubber sheets (Rubber Sheet Roll, Amazon.com) were cut into rectangular pieces with scissors. The top surfaces were treated with poly-L-lysine to improve adhesion. A solution containing *B. subtilis* spores was placed on pieces of rubber sheet and then allowed to dry in a fume hood. The relative humidity of the laboratory air was ~15–20%. The amount of solution to be placed on the rubber sheet was determined by visually inspecting the spore coverage under an optical microscope. Once the solution had dried, the rubber sheets already exhibited a curvature because the relative humidity of the laboratory air was low (~15–20%). The sheets were then placed in a chamber with saturated air and kept there for a day. This procedure increased the curvature of the rubber sheets once they were placed back in low relative humidity.

Measurement of plane stress and radius of curvature of the rubber sheet. The rubber sheet was cut into a 2 × 6 cm rectangular piece and coated with a layer of spores. The sheet was attached, at its centre, to a piece of acrylic glass with adhesive tape and then placed vertically in a humidity chamber with transparent walls. The relative humidity inside the chamber was monitored with a hygrometer (Vaisala). The chamber relative humidity was gradually increased from the laboratory level (~18% at the time of the measurements) by supplying saturated air. Photographs of the latex sheet were taken from a direction that allowed the 2-cm-wide edge to be seen. Pictures were taken at intervals of 5% relative humidity, starting at 20%.

The plane stress at the spore layer was determined according to the formula

$$\sigma_x = \frac{Et^2}{6(1-\nu^2)}\left(\frac{1}{R_x} - \nu\frac{1}{R_y}\right) \quad (2)$$

where σ_x is the surface stress along the direction of the observed curvature, E is Young's modulus of rubber, ν is Poisson's coefficient for rubber, t is the thickness of the rubber sheet and R_x, R_y are the radii of the curvature. t is 0.5 mm for the sheet used in Fig. 3. R_x is estimated by fitting the optical pictures of the rubber with a circle. R_y is assumed to be infinite because the rubber sheet exhibited a cylindrical shape. Strain at the surface of the rubber sheet near the spores is estimated from $2t/3R_x$ (the neutral plane is $2t/3$ below the surface, see also equations (2.3)–(2.6) of ref. 9). We determined E from the stress–strain curves for a rectangular strip of the same latex rubber sample (1.3 MPa). ν is taken as 0.5. Note that in contrast to equation (1), equation (2) accounts for anisotropic stresses in the spore layer. The cylindrical geometry of the rubber sheet originated during the spore drying. This shape was stable.

Experimental set-up for electricity generation. A 0.750-mm-thick latex rubber sheet, 5 × 8 cm, was coated with a layer of *B. subtilis* spores. The sheet was brought into physical contact with one end of a lever that pivoted around a central axis like a seesaw. We connected the opposite end of the lever to an electromagnetic generator with a short string. The electromagnetic generator consisted of a stack of magnets rotating between two copper coils. Copper coils were formed by winding a total of 6,705.6 m of 42-gauge magnet wire (Polytech Coil Winding). The magnet stack was composed of two 5.08 × 1.27 × 0.635 cm and two 5.08 × 1.27 × 0.3175 cm neodymium magnets. We used silicon nitride ball bearings to allow the magnets to rotate with respect to the coils.

The container used to hold water was 9 cm wide along the direction parallel to the 8-cm-long edge of the spore-coated latex sheet. The length and depth of the container were 15 cm and 4 cm, respectively. Aluminium foil was placed 1.5 cm above the water-filled container so that water vapour could leave only from the 9-cm-wide sides, as shown in Fig. 3a. The container was placed on a ceramic-top heater (Corning, PC-600D). The temperature of the water was monitored with a digital thermometer and kept at 31 °C. The room temperature and relative humidity were ~24 °C and 30%, respectively. We used a low-power d.c. electric fan to create air flow. The fan was placed either close to the 1.5-cm-wide opening of the water container to transport moisture to the device, or away from the opening to transport dry air to the device. A hot wire anemometer (Cole-Palmer, EW-30005-85)

measured the air velocity in the vicinity of the latex rubber sheet to be less than 0.5 m s^{-1} in either position of the electric fan. Measurements with an empty container showed that the background power induced by the air flow was ~3.5 nW.

Received 30 April 2013; accepted 3 December 2013; published online 26 January 2014

References

1. Stuart, M. A. C. *et al.* Emerging applications of stimuli-responsive polymer materials. *Nature Mater.* **9,** 101–113 (2010).
2. Yashin, V. V. & Balazs, A. C. Pattern formation and shape changes in self-oscillating polymer gels. *Science* **314,** 798–801 (2006).
3. Wheeler, T. D. & Stroock, A. D. The transpiration of water at negative pressures in a synthetic tree. *Nature* **455,** 208–212 (2008).
4. He, X. *et al.* Synthetic homeostatic materials with chemo-mechano-chemical self-regulation. *Nature* **487,** 214–218 (2012).
5. Sidorenko, A., Krupenkin, T., Taylor, A., Fratzl, P. & Aizenberg, J. Reversible switching of hydrogel-actuated nanostructures into complex micropatterns. *Science* **315,** 487–490 (2007).
6. Madden, J. D. W. *et al.* Artificial muscle technology: physical principles and naval prospects. *IEEE J. Ocean. Eng.* **29,** 706–728 (2004).
7. Ma, M., Guo, L., Anderson, D. G. & Langer, R. Bio-inspired polymer composite actuator and generator driven by water gradients. *Science* **339,** 186–189 (2013).
8. Kim, H. & Kwon, S. Water-responsive polymer composites on the move. *Science* **339,** 150–151 (2013).
9. Reyssat, E. & Mahadevan, L. Hygromorphs: from pine cones to biomimetic bilayers. *J. R. Soc. Interface* **6,** 951–957 (2009).
10. Reyssat, E. & Mahadevan, L. How wet paper curls. *Europhys. Lett.* **93,** 54001 (2011).
11. Pickard, W. F. The ascent of sap in plants. *Prog. Biophys. Mol. Biol.* **37,** 181–229 (1981).
12. Hacke, U. G., Sperry, J. S., Pockman, W. T., Davis, S. D. & McCulloh, K. A. Trends in wood density and structure are linked to prevention of xylem implosion by negative pressure. *Oecologia* **126,** 457–461 (2001).
13. Dawson, J., Vincent, J. F. V. & Rocca, A. M. How pine cones open. *Nature* **390,** 668 (1997).
14. Elbaum, R., Zaltzman, L., Burgert, I. & Fratzl, P. The role of wheat awns in the seed dispersal unit. *Science* **316,** 884–886 (2007).
15. Fratzl, P. & Barth, F. G. Biomaterial systems for mechanosensing and actuation. *Nature* **462,** 442–448 (2009).
16. Nicholson, W. L., Munakata, N., Horneck, G., Melosh, H. J. & Setlow, P. Resistance of *Bacillus* endospores to extreme terrestrial and extraterrestrial environments. *Microbiol. Mol. Biol. Rev.* **64,** 548–572 (2000).
17. Westphal, A. J., Price, P. B., Leighton, T. J. & Wheeler, K. E. Kinetics of size changes of individual *Bacillus thuringiensis* spores in response to changes in relative humidity. *Proc. Natl Acad. Sci. USA* **100,** 3461–3466 (2003).
18. Driks, A. The dynamic spore. *Proc. Natl Acad. Sci. USA* **100,** 3007–3009 (2003).
19. Plomp, M., Leighton, T., Wheeler, K. E. & Malkin, A. J. The high-resolution architecture and structural dynamics of *Bacillus* spores. *Biophys. J.* **88,** 603–608 (2004).
20. Sahin, O., Yong, E. H., Driks, A. & Mahadevan, L. Physical basis for the adaptive flexibility of *Bacillus* spore coats. *J. R. Soc. Interface* **9,** 3156–3160 (2012).
21. Driks, A., Roels, S., Beall, B., Moran, C. P. J. & Losick, R. Subcellular localization of proteins involved in the assembly of the spore coat of *Bacillus subtilis*. *Genes Dev.* **8,** 234–244 (1994).
22. Buehler, M. J. & Yung, Y. C. Deformation and failure of protein materials in physiologically extreme conditions and disease. *Nature Mater.* **8,** 175–188 (2009).
23. Whaley, S. R., English, D. S., Hu, E. L., Barbara, P. F. & Belcher, A. M. Selection of peptides with semiconductor binding specificity for directed nanocrystal assembly. *Nature* **405,** 665–668 (2000).
24. Lee, B. Y. *et al.* Virus-based piezoelectric energy generation. *Nature Nanotech.* **7,** 351–356 (2012).
25. Driks, A. & Mallozzi, M. in *Bacillus anthracis and Anthrax* (ed. N. Bergman) 17–38 (Wiley, 2009).
26. Timoshenko, S. Analysis of bi-metal thermostats. *Rev. Sci. Instrum.* **11,** 233–255 (1925).
27. Paradiso, J. A. & Starner, T. Energy scavenging for mobile and wireless electronics. *IEEE Pervasive Comput.* **4,** 18–27 (2005).
28. Wang, Z. L. & Song, J. Piezoelectric nanogenerators based on zinc oxide nanowire arrays. *Science* **312,** 242–246 (2006).
29. Hong, H. A., Duc, L. H. & Cutting, S. M. The use of bacterial spore formers as probiotics. *FEMS Microbiol. Rev.* **29,** 813–835 (2005).
30. Sader, J. E., Chon, J. W. & Mulvaney, P. Calibration of rectangular atomic force microscope cantilevers. *Rev. Sci. Instrum.* **70,** 3967 (1999).

Acknowledgements

This work is supported by the US Department of Energy (DOE), Office of Science, Basic Energy Sciences (BES), under award no. DE-SC0007999 (spore energy density measurements), the Rowland Junior Fellows Program (bio-hybrid hygromorph actuators), and the Wyss Institute for Biologically Inspired Engineering (hygrovoltaic generators). The authors thank D. E. Ingber for encouragement and comments on the manuscript, C. P. Stokes for help with the experimental set-up for rapidly switching the humidity levels surrounding the spores, D. Bell for help with electron microscopy and J. M. Sungur for prototype device manufacturing.

Author contributions

X.C. performed the experiments in Fig. 1 and analysed the data. L.M. contributed to the theory and scaling estimates. A.D. contributed mutant and wild-type spore samples. O.S. conceived and designed the experiments and performed the experiments in Figs 2 and 3. O.S. and L.M. wrote the paper.

Additional information

Supplementary information is available in the online version of the paper. Reprints and permissions information is available online at www.nature.com/reprints. Correspondence and requests for materials should be addressed to O.S.

Competing financial interests

A patent application has been filed by Harvard University. US provisional application no. 61/415,902: 'Bacterial spore based energy system'.